Published in final edited form as:

J Am Chem Soc. 2020 April 15; 142(15): 6896–6901. doi:10.1021/jacs.0c01314.

Reversible Switching between Nonporous and Porous Phases of a New SIFSIX Coordination Network Induced by a Flexible Linker Ligand

Bai-Qiao Song,
Department of Chemical Sciences and Bernal Institute, University of Limerick, Limerick V94 T9PX, Republic of Ireland

Qing-Yuan Yang,
School of Chemical Engineering and Technology, Xi'an Jiaotong University, Xi'an 710049, China

Shi-Qiang Wang,
Department of Chemical Sciences and Bernal Institute, University of Limerick, Limerick V94 T9PX, Republic of Ireland

Matthias Vandichel,
Department of Chemical Sciences and Bernal Institute, University of Limerick, Limerick V94 T9PX, Republic of Ireland

Amrit Kumar,
Department of Chemical Sciences and Bernal Institute, University of Limerick, Limerick V94 T9PX, Republic of Ireland

Clare Crowley,
Department of Chemical Sciences and Bernal Institute, University of Limerick, Limerick V94 T9PX, Republic of Ireland

Naveen Kumar,
Department of Chemical Sciences and Bernal Institute, University of Limerick, Limerick V94 T9PX, Republic of Ireland

Cheng-Hua Deng,

Corresponding Author: Michael J. Zaworotko – Department of Chemical Sciences and Bernal Institute, University of Limerick, Limerick V94 T9PX, Republic of Ireland; Michael.Zaworotko@ul.ie.

ASSOCIATED CONTENT

Supporting Information

The Supporting Information is available free of charge at https://pubs.acs.org/doi/10.1021/jacs.0c01314.

Materials and methods, supporting figures, supporting tables, and supporting references (PDF)

Crystallographic information file (CIF)

Crystallographic information file (CIF)

Crystallographic information file (CIF)

Crystallographic information file (CIF)

Crystallographic information file (CIF)

(CIF)

Complete contact information is available at: https://pubs.acs.org/10.1021/jacs.0c01314

The authors declare no competing financial interest.

Department of Chemical Sciences and Bernal Institute, University of Limerick, Limerick V94 T9PX, Republic of Ireland

Victoria GasconPerez,
Department of Chemical Sciences and Bernal Institute, University of Limerick, Limerick V94 T9PX, Republic of Ireland

Matteo Lusi,
Department of Chemical Sciences and Bernal Institute, University of Limerick, Limerick V94 T9PX, Republic of Ireland

Hui Wu,
NIST Center for Neutron Research, National Institute of Standards and Technology, Gaithersburg, Maryland 20899-6102, United States

Wei Zhou,
NIST Center for Neutron Research, National Institute of Standards and Technology, Gaithersburg, Maryland 20899-6102, United States

Michael J. Zaworotko
Department of Chemical Sciences and Bernal Institute, University of Limerick, Limerick V94 T9PX, Republic of Ireland

Abstract

Closed-to-open structural transformations in flexible coordination networks are of potential utility in gas storage and separation. Herein, we report the first example of a flexible SiF_6^{2-}-pillared square grid material, $[Cu(SiF_6)(L)_2]_n$ (L = 1,4-bis(1-imidazolyl)benzene), SIFSIX-23-Cu. SIFSIX-23-Cu exhibits reversible switching between nonporous (β1) and several porous (α, γ1, γ2, and γ3) phases triggered by exposure to N_2, CO_2, or H_2O. In addition, heating β1 to 433 K resulted in irreversible transformation to a closed polymorph, β2. Single-crystal X-ray diffraction studies revealed that the phase transformations are enabled by rotation and geometrical contortion of L. Density functional theory calculations indicated that L exhibits a low barrier to rotation (as low as 8 $kJmol^{-1}$) and a rather flat energy surface. In situ neutron powder diffraction studies provided further insight into these sorbate-induced phase changes. SIFSIX-23-Cu combines stability in water for over a year, high CO_2 uptake (ca. 216 cm^3/g at 195 K), and good thermal stability.

Metal–organic materials (MOMs)[1] such as metal–organic frameworks (MOFs)[2] and porous coordination polymers (PCPs)[3] offer potential solutions to the high-energy footprint, costs, and risks associated with storage or purification of gases and vapors.[4] Whereas rigid microporous MOMs typically display type I isotherms, flexible MOMs (FMOMs)[5] can exhibit stepped isotherms from structural contraction (expansion) under reduced (increased) pressure, i.e., breathing or swelling.[6] FMOMs that exhibit stepped type F–IV isotherms, sudden switching from a nonporous (closed) activated phase to a porous (open) phase, are of particular interest for pressure swing adsorption (PSA) gas storage,[7] as negligible adsorbate is present at low pressure.[8] Closed-to-open transformations might also facilitate gas separation if adsorbates selectively induce transformations.[9] Thus far, only ca. 150 FMOMs

of the >20 000 porous MOMs reported are known to be flexible,[5b,10] and just a handful exhibit type F-IV isotherms with saturated uptake of >200 cm^3/g.[11] None of these high-uptake FMOMs are sustained by inorganic linker ligands, a matter we address herein.

The “pillared sheet” platform of materials comprised of cationic square grid lattice (sql) sheets and hexafluorosilicate (SiF_6^{2-}, “SIFSIX”) pillars[12] exhibit benchmark performance with respect to separation of industrial gases such as CO_2, SO_2, and small-molecule hydrocarbons.[13] Whereas modeling studies indicate that rotation of pyrazine rings in SIFSIX-3-M (M = Ni, Fe) can cause inflections in Xe adsorption isotherms, the framework remains rigid.[14] SIFSIX nets can also transform into nonporous sql or sql-c* nets under humid conditions.[15] Herein, we introduce the first flexible SIFSIX net, $[Cu(SiF_6)\text{-}(L)_2]_n$ (L = 1,4-bis(1-imidazolyl)benzene), **SIFSIX-23-Cu** (Figure 1).

Layering 1:1 MeOH/H_2O onto $CuSiF_6$ in H_2O followed by further layering of a solution of L in MeOH afforded purple, needle-shaped crystals of **SIFSIX-23-Cu**·*x*MeOH·*y*H_2O (see Supporting Information (SI)), **SIFSIX-23-Cu-*α***. Cu(II) cations are octahedrally coordinated to four equatorial L ligands (two L(*syn*) and two L(*anti*)), while SIFSIX anions occupy the axial sites to afford a noninterpenetrated pcu topology framework (Figure 1a). The CuL_2 sql net undulates due to out-of-plane protrusion of “V”-shaped L(*syn*) linker ligands. The pillars adopt a *cis*-bridging mode, unlike other coordination networks involving SIFSIX anions (Figures S1 and S2).[12,13,16] **SIFSIX-23-Cu-*α*** possesses a 1D channel of diameter 5.4 × 4.0 $Å^2$ along the *a*-axis (Figure 1b) with a calculated accessible void volume of 41.8% (Figure S3).

We found that desolvation induces **SIFSIX-23-Cu-*α*** to undergo multiple phase transformations to **SIFSIX-23-Cu-*γ*1**, **-*γ*2**, **-*γ*3**, and a solvent-free closed form, **SIFSIX-23-Cu-*β*1** (Figures 2a and S4, Table S1). Whereas the space group and unit cell parameters vary, the connectivity of the **SIFSIX-23-Cu** network is preserved even with extreme deformation (Figure 2b, Table S2). The ***α*** to ***γ*3** transformation caused the parallelogram of the sql net to undergo hinge-like motion with negligible change in edge length (Δd_{max} = 0.2 Å) but a decrease in ∠Cu–Cu–Cu from 90° (***α***) to 53.4° (***γ*3**) (Figure 2b and c). Concomitantly, one diagonal of the parallelogram reduced from 18.46 Å (***α***) to 11.67 Å (***γ*3**), whereas the other expanded from 18.46 Å (***α***) to 23.19 Å (***γ*3**). An overall reduction in guest-accessible volume from 41.8% (***α***) to 20.4% (***γ*3**) was calculated by PLATON.[17] Removal of solvent from ***γ*3** afforded **SIFSIX-23-Cu-*β*1**, a nonporous phase (Figures 2b and S5 and S6) with 34.5% volume reduction vs the ***α*** phase. The transformation from ***γ*3** to ***β*1** differs from the other phase changes (Figure 2b and d). FMOMs rarely exhibit such extreme structural changes.[11] ***β*1** reverted to ***α*** after immersion in MeOH, EtOH, or CH_3CN (Figure S7).

Structural analysis of the **SIFSIX-23-Cu** phases (Figures 2e and S8–S11, Table S2 and S3)[18] reveals hinge-like motion in the ***α*** to ***γ*1** transformation that originates from rotation of imidazolyl rings and reorientation of phenyl rings. Indeed, rotation of L is a feature of each transformation (Figure S8). In the ***γ*1** to ***β*1** transformation, the coordinated N atom acts as a hinge or “kneecap” at which the Cu-imidazolyl junction bends (Figure S9). For the ***γ*3** to ***β*1** transformation, one imidazolyl ring of L(*syn*) bends at the $N(1)_{imidazolyl}$ atom to subtend an

angle of 16.9° between the C_{phenyl}–$N_{imidazolyl}$ bond and the imidazolyl plane (Figure S10),[8d,11d,19] enabling shrinkage of the Cu–L(*syn*)–Cu edge in **β1**. These structural changes are mainly associated with L(*syn*) (Figure S11). C–H···F hydrogen bonds between SIFSIX anions and CH moieties of aromatic groups (Table S4) are often present in SIFSIX coordination networks (Figure S12).[13] Density functional theory (DFT) calculations indicated that L exhibits a low rotational barrier (<8 kJ/mol) and a rather flat energy surface with minima corresponding to L(*syn*) and L(*anti*). A Cambridge Structural Database (CSD)[20] survey revealed that dihedral angles between phenyl and imidazolyl rings are consistent with those in L(*syn*) and L(*anti*) (Figures S13–S15). The energy difference of L(*syn*) calculated before and after bending from **γ3** to **β1** is also small (<16 kJ/mol) (Figure S16). The nature of L helps to explain the "softness" of **SIFSIX-23-Cu**.[21]

Variable-temperature PXRD studies of the **α** to **β1** transformation (Figures 3a and S17) revealed a new phase at 425 K as also suggested by DSC (Figure 3b). That no weight loss was seen in the corresponding TGA curve indicates that this was a temperature-controlled rather than guest-controlled transformation. Heating **β1** or any of the **α** phases at 433 K afforded single crystals of **SIFSIX-23-Cu-β2**. Single-crystal X-ray diffraction (SCXRD) characterization revealed that **β2** exhibits a slightly smaller cell volume than that of **β1**. The connectivity is unchanged if *anti*-to-*syn* switching of L(*anti*) and swing motion of SIFSIX anions (Figure 3c) had occurred. That **β2** is more stable than **β1** is supported by its higher density, structural parameters which suggest less strain (Figure S11) and lack of reversibility after immersion in water, MeOH, EtOH, or CH_3CN (Figure S18) and periodic DFT calculations (PBE and PBE-dDsC). The DFT calculations revealed that small global energy differences between the **α** to **γ3** phases (Figure 3d) are consistent with the reversibility of the structural transformations (Table S5, Figure S19). The energy difference between **β1** and **γ3** is 86.7 kJ/mol, a value that can be offset by adsorption. The **β2** phase was determined to be relatively more stable (−222 kJ/mol vs **α**).

Since the closed-to-open transformation from **β1** to **α** was induced by solvent, we anticipated that gases might also trigger switching. The CO_2 isotherm of **β1** at 195 K indeed displayed switching with two steps (Figure 4a). The first step at ca. 2.4 mmHg (adsorbed CO_2 = 84 cm^3/g) gave a micropore volume of 0.16 cm^3/g, close to that estimated from the crystal structure of **γ3** (0.15 cm^3/g). The second step occurred after saturation (ca. 216 cm^3/g) with a micropore volume of 0.40 cc/g, in good agreement with the structure of **α** (0.40 cm^3/g). The Langmuir surface areas for the phases in the first and second steps calculated from the CO_2 isotherm at 195 K are 451 and 941 $m^2\ g^{-1}$, respectively (Figures S20 and S21). **β1** also displayed gate opening for N_2 at 77 K with an onset pressure of 142 mmHg and saturated uptake of 160 cm^3/g at 738 mmHg (Figure 4a). In contrast, the N_2 (77 K) and CO_2 (195 K) isotherms for **β2** revealed no uptake (Figure S22).

In situ neutron powder diffraction (NPD) data were collected under various conditions to further study these switching events (Figure 4e). The diffraction pattern obtained at 0 bar matched that calculated for **β1**. For P = 0.02 bar at 195 K (the first step), the NPD pattern resembled that calculated for **γ3**. For P = 0.2 bar (the second step), the NPD pattern matched that calculated for **α**. The **α** phase reverted to **β1** at P = 0 bar and 298 K. NPD data of samples collected at 77 K under 1 bar N_2 validated the formation of **α**. The saturated uptake

of N_2 was lower than that calculated from the pore volume based on the CO_2 sorption data (258 cm^3/g), perhaps because at 77 K sorbate–sorbent interactions are strong enough to hinder diffusion.[22] This guest-dependent switching behavior suggests that structural transformations are driven by host–guest interactions.

The low-pressure CO_2 sorption isotherms at near ambient temperature revealed no switching behavior induced by CO_2 at 298 K below 1 bar (Figures 4b and S23). However, **β1** exhibited a single step type F-IV isotherm at 273 K with a gate-opening pressure of 505 mmHg and saturated uptake of 77 cm^3/g at 759 mmHg. The corresponding desorption isotherm displayed hysteresis. The calculated micropore volume of 0.15 cm^3/g agrees with that calculated from the crystal structure of **γ3** (0.15 cm^3/g). In situ NPD data collected at 273 K and 1 bar CO_2 showed a similar NPD pattern to that obtained at 195 K for 0.02 bar CO_2, i.e., the **γ3** phase (Figure 4e). That this phase switching is reversible was demonstrated by 41 cycles of CO_2 adsorption/desorption (Figures 4c and S24–S26). PXRD confirmed structural integrity (Figure S27). CO_2 triggered closed to open switching with an onset gate-opening pressure of <1 bar at 273 K observed in the ELM family of materials and zeolitic imidazolate frameworks (ZIFs).[8b,23]

High-pressure CO_2 sorption on **β1** (Figure 4d) resembled the isotherm obtained at 195 K. The onset gate-opening pressures for the first and second step at 298 K are around 2 and 5.8 bar, respectively. Interestingly, even at 55 °C CO_2 triggers gate-opening with a threshold pressure of *ca*. 5.3 bar, a pressure suitable for high-temperature gas sorption and separation. CO_2-induced closed-to-open switching from **β1** to **α** at high pressure was found to be reversible (Figures S28–S30).

SIFSIX-23-Cu-β1 also underwent closed-to-open switching induced by water vapor at 298 K (Figure 4f). The steep water uptake (2.8%) at low humidity matches the SCXRD results, which indicate that **β1** can capture one water molecule without a structural change. **β1** sequentially formed **γ3**, **γ2**, and **γ1** under atmospheric humidity (Figures S31 and S32) whereas water immersion caused **β1** to revert to **α** (Figures S7). **SIFSIX-23-Cu-α** retained single-crystallinity after immersion in water for one year (Figures 5 and S33 and S34). This strong hydrolytic stability contrasts with that of other SIFSIX materials.[15]

In summary, the new pillared square grid coordination network **SIFSIX-23-Cu** exhibits an uncommon *cis*-bridging coordination mode of SIFSIX anions and is to our knowledge the first hybrid coordination network that undergoes reversible guest-induced closed-to-open transformations. It is also one of the highest uptake materials with a type F-IV isotherm. We attribute these facile and reversible transformations to the low rotational barrier of L and the correspondingly flat energy surface.

Supplementary Material

Refer to Web version on PubMed Central for supplementary material.

ACKNOWLEDGMENTS

We gratefully acknowledge Science Foundation Ireland (SFI Awards 13/RP/B2549 and 16/IA/4624) and the Irish Research Council (IRCLA/2019/167).

REFERENCES

(1). Perry JJ IV; Perman JA; Zaworotko MJ Design and synthesis of metal–organic frameworks using metal–organic polyhedra as supermolecular building blocks. Chem. Soc. Rev 2009, 38, 1400. [PubMed: 19384444]

(2). (a)Furukawa H; Cordova KE; O'Keeffe M; Yaghi OM The Chemistry and Applications of Metal-Organic Frameworks. Science 2013, 341, 1230444. [PubMed: 23990564] (b)Farrusseng D Metal-Organic Frameworks: Applications from Catalysis to Gas Storage; Wiley, 2011.

(3). (a)Kitagawa S; Kitaura R; Noro S-I Functional Porous Coordination Polymers. Angew. Chem., Int. Ed 2004, 43, 2334.(b)Batten SR; Neville SM; Turner DR Coordination Polymers: Design, Analysis and Application; The Royal Society of Chemistry: Cambridge, U.K., 2009.

(4). (a)Adil K; Belmabkhout Y; Pillai RS; Cadiau A; Bhatt PM; Assen AH; Maurin G; Eddaoudi M Gas/vapour separation using ultra-microporous metal–organic frameworks: insights into the structure/separation relationship. Chem. Soc. Rev 2017, 46, 3402. [PubMed: 28555216] (b)Kitagawa S Porous Materials and the Age of Gas. Angew. Chem., Int. Ed 2015, 54, 10686. (c)Lin R-B; Xiang S; Xing H; Zhou W; Chen B Exploration of porous metal–organic frameworks for gas separation and purification. Coord. Chem. Rev 2019, 378, 87.

(5). (a)Horike S; Shimomura S; Kitagawa S Soft porous crystals. Nat. Chem 2009, 1, 695. [PubMed: 21124356] (b)Schneemann A; Bon V; Schwedler I; Senkovska I; Kaskel S; Fischer RA Flexible metal–organic frameworks. Chem. Soc. Rev 2014, 43, 6062. [PubMed: 24875583] (c)Féerey G Hybrid porous solids: past, present, future. Chem. Soc. Rev 2008, 37, 191. [PubMed: 18197340] (d)Murdock CR; Hughes BC; Lu Z; Jenkins DM Approaches for synthesizing breathing MOFs by exploiting dimensional rigidity. Coord. Chem. Rev 2014, 258–259, 119.

(6). (a)Zhou D-D; Chen P; Wang C; Wang S-S; Du Y; Yan H; Ye Z-M; He C-T; Huang R-K; Mo Z-W; Huang N-Y; Zhang J-P Intermediate-sized molecular sieving of styrene from larger and smaller analogues. Nat. Mater 2019, 18, 994. [PubMed: 31308517] (b)Zhang Y; Zhang X; Lyu J; Otake K.-i.; Wang X; Redfern LR; Malliakas CD; Li Z; Islamoglu T; Wang B; Farha OK A Flexible Metal–Organic Framework with 4-Connected Zr6 Nodes. J. Am. Chem. Soc 2018, 140, 11179. [PubMed: 30113833] (c)Rabone J; Yue Y-F; Chong SY; Stylianou KC; Bacsa J; Bradshaw D; Darling GR; Berry NG; Khimyak YZ; Ganin AY; Wiper P; Claridge JB; Rosseinsky MJ An Adaptable Peptide-Based Porous Material. Science 2010, 329, 1053. [PubMed: 20798314] (d)Katsoulidis AP; Antypov D; Whitehead GFS; Carrington EJ; Adams DJ; Berry NG; Darling GR; Dyer MS; Rosseinsky MJ Chemical control of structure and guest uptake by a conformationally mobile porous material. Nature 2019, 565, 213. [PubMed: 30626943] (e)Carrington EJ; McAnally CA; Fletcher AJ; Thompson SP; Warren M; Brammer L Solvent-switchable continuous-breathing behaviour in a diamondoid metal–organic framework and its influence on CO2 versus CH4 selectivity. Nat. Chem 2017, 9, 882. [PubMed: 28837170] (f)Xiao B; Byrne PJ; Wheatley PS; Wragg DS; Zhao X; Fletcher AJ; Thomas KM; Peters L; Evans JSO; Warren JE; Zhou W; Morris RE Chemically blockable transformation and ultraselective low-pressure gas adsorption in a non-porous metal organic framework. Nat. Chem 2009, 1, 289. [PubMed: 21495253] (g)Shivanna M; Yang Q-Y; Bajpai A; Patyk-Kazmierczak E; Zaworotko MJ A dynamic and multi-responsive porous flexible metal–organic material. Nat. Commun 2018, 9, 3080. [PubMed: 30082776] (h)Serre C; Mellot-Draznieks C; Surble S; Audebrand N; Filinchuk Y; Férey G Role of Solvent-Host Interactions That Lead to Very Large Swelling of Hybrid Frameworks. Science 2007, 315, 1828. [PubMed: 17395825] (i)Serre C; Millange F; Thouvenot C; Noguès M; Marsolier G; Louër D; Féerey G Very Large Breathing Effect in the First Nanoporous Chromium(III)-Based Solids: MIL-53 or CrIII-(OH)·{O2C-C6H4-CO2}·{HO2C-C6H4-CO2H}x·H2Oy. J. Am. Chem. Soc 2002, 124, 13519. [PubMed: 12418906]

(7). (a)Sakaida S; Otsubo K; Sakata O; Song C; Fujiwara A; Takata M; Kitagawa H Crystalline coordination framework endowed with dynamic gate-opening behaviour by being downsized to a thin film. Nat. Chem 2016, 8, 377. [PubMed: 27001734] (b)Jin J; Zhao X; Feng P; Bu X A

Cooperative Pillar–Template Strategy as a Generalized Synthetic Method for Flexible Homochiral Porous Frameworks. Angew. Chem 2018, 130, 3799.(c)Engel ER; Jouaiti A; Bezuidenhout CX; Hosseini MW; Barbour LJ Activation-Dependent Breathing in a Flexible Metal–Organic Framework and the Effects of Repeated Sorption/Desorption Cycling. Angew. Chem., Int. Ed 2017, 56, 8874.(d)Hazra A; van Heerden DP; Sanyal S; Lama P; Esterhuysen C; Barbour LJ CO2-induced single-crystal to single-crystal transformations of an interpenetrated flexible MOF explained by in situ crystallographic analysis and molecular modeling. Chem. Sci 2019, 10, 10018. [PubMed: 32015814]

(8). (a)Wharmby MT; Henke S; Bennett TD; Bajpe SR; Schwedler I; Thompson SP; Gozzo F; Simoncic P; Mellot-Draznieks C; Tao H; Yue Y; Cheetham AK Extreme Flexibility in a Zeolitic Imidazolate Framework: Porous to Dense Phase Transition in Desolvated ZIF-4. Angew. Chem., Int. Ed 2015, 54, 6447.(b)McGuirk CM; Runčevski T; Oktawiec J; Turkiewicz A; Taylor MK; Long JR Influence of Metal Substitution on the Pressure-Induced Phase Change in Flexible Zeolitic Imidazolate Frameworks. J. Am. Chem. Soc 2018, 140, 15924. [PubMed: 30403480] (c)Kundu T; Wahiduzzaman M; Shah BB; Maurin G; Zhao D Solvent-Induced Control over Breathing Behavior in Flexible Metal–Organic Frameworks for Natural-Gas Delivery. Angew. Chem., Int. Ed 2019, 58, 8073.(d)Yang H; Guo F; Lama P; Gao W-Y; Wu H;Barbour LJ; Zhou W; Zhang J; Aguila B; Ma S Visualizing Structural Transformation and Guest Binding in a Flexible Metal–Organic Framework under High Pressure and Room Temperature. ACS Cent. Sci 2018, 4, 1194. [PubMed: 30276253]

(9). (a)Gücüyener C; van den Bergh J; Gascon J; Kapteijn F Ethane/Ethene Separation Turned on Its Head: Selective Ethane Adsorption on the Metal-Organic Framework ZIF-7 through a Gate-Opening Mechanism. J. Am. Chem. Soc 2010, 132, 17704. [PubMed: 21114318] (b)Nijem N; Wu H; Canepa P; Marti A; Balkus KJ; Thonhauser T; Li J; Chabal YJ Tuning the Gate Opening Pressure of Metal–Organic Frameworks (MOFs) for the Selective Separation of Hydrocarbons. J. Am. Chem. Soc 2012, 134, 15201. [PubMed: 22946693] (c)Taylor MK; Runčevski T; Oktawiec J; Bachman JE; Siegelman RL; Jiang H; Mason JA; Tarver JD; Long JR Near-Perfect CO2/CH4 Selectivity Achieved through Reversible Guest Templating in the Flexible Metal–Organic Framework Co(bdp). J. Am. Chem. Soc 2018, 140, 10324. [PubMed: 30032596] (d)Wang S-Q; Mukherjee S; Patyk-Kaźmierczak E; Darwish S; Bajpai A; Yang Q-Y; Zaworotko MJ Highly Selective, High-Capacity Separation of o-Xylene from C8 Aromatics by a Switching Adsorbent Layered Material. Angew. Chem 2019, 131, 6702.

(10). Moghadam PZ; Li A; Wiggin SB; Tao A; Maloney AGP; Wood PA; Ward SC; Fairen-Jimenez D Development of a Cambridge Structural Database Subset: A Collection of Metal–Organic Frameworks for Past, Present, and Future. Chem. Mater 2017, 29, 2618.

(11). (a)Mason JA; Oktawiec J; Taylor MK; Hudson MR; Rodriguez J; Bachman JE; Gonzalez MI; Cervellino A; Guagliardi A; Brown CM; Llewellyn PL; Masciocchi N; Long JR Methane storage in flexible metal–organic frameworks with intrinsic thermal management. Nature 2015, 527, 357. [PubMed: 26503057] (b)Klein N; Hoffmann HC; Cadiau A; Getzschmann J; Lohe MR; Paasch S; Heydenreich T; Adil K; Senkovska I; Brunner E; Kaskel S Structural flexibility and intrinsic dynamics in the M2(2,6-ndc)2-(dabco) (M = Ni, Cu, Co, Zn) metal–organic frameworks. J. Mater. Chem 2012, 22, 10303.(c)Zhu A-X; Yang Q-Y; Kumar A; Crowley C; Mukherjee S; Chen K-J; Wang S-Q; O′Nolan D; Shivanna M; Zaworotko MJ Coordination Network That Reversibly Switches between Two Nonporous Polymorphs and a High Surface Area Porous Phase. J. Am. Chem. Soc 2018, 140, 15572. [PubMed: 30395458] (d)Yang Q-Y; Lama P; Sen S; Lusi M; Chen K-J; Gao W-Y; Shivanna M; Pham T; Hosono N; Kusaka S; Perry JJ IV; Ma S; Space B; Barbour LJ; Kitagawa S; Zaworotko MJ Reversible Switching between Highly Porous and Nonporous Phases of an Interpenetrated Diamondoid Coordination Network That Exhibits Gate-Opening at Methane Storage Pressures. Angew. Chem., Int. Ed 2018, 57, 5684.(e)Zhu A-X; Yang Q-Y; Mukherjee S; Kumar A; Deng C-H; Bezrukov AA; Shivanna M; Zaworotko MJ Tuning the Gate-Opening Pressure in a Switching pcu Coordination Network, X-pcu-5-Zn, by Pillar-Ligand Substitution. Angew. Chem., Int. Ed 2019, 58, 18212.(f)Chen L; Mowat JPS; Fairen-Jimenez D; Morrison CA; Thompson SP; Wright PA; Düren T Elucidating the Breathing of the Metal–Organic Framework MIL-53(Sc) with ab Initio Molecular Dynamics Simulations and in Situ X-ray Powder Diffraction Experiments. J. Am. Chem. Soc 2013, 135, 15763. [PubMed: 23731240] (g)Seo J; Matsuda R; Sakamoto H; Bonneau C; Kitagawa S A Pillared-Layer Coordination

Polymer with a Rotatable Pillar Acting as a Molecular Gate for Guest Molecules. J. Am. Chem. Soc 2009, 131, 12792. [PubMed: 19681608]

(12). Subramanian S; Zaworotko MJ Porous Solids by Design: [Zn(4,4′-bpy)2(SiF6)]n·xDMF, a Single Framework Octahedral Coordination Polymer with Large Square Channels. Angew. Chem., Int. Ed. Engl 1995, 34, 2127.

(13). (a)Nugent P; Belmabkhout Y; Burd SD; Cairns AJ; Luebke R; Forrest K; Pham T; Ma S; Space B; Wojtas L; Eddaoudi M; Zaworotko MJ Porous materials with optimal adsorption thermodynamics and kinetics for CO2 separation. Nature 2013, 495, 80. [PubMed: 23446349] (b)Cui X; Chen K; Xing H; Yang Q; Krishna R; Bao Z; Wu H; Zhou W; Dong X; Han Y; Li B; Ren Q; Zaworotko MJ; Chen B Pore chemistry and size control in hybrid porous materials for acetylene capture from ethylene. Science 2016, 353, 141. [PubMed: 27198674] (c)Chen K-J; Madden DG; Mukherjee S; Pham T; Forrest KA; Kumar A; Space B; Kong J; Zhang Q-Y; Zaworotko MJ Synergistic sorbent separation for one-step ethylene purification from a four-component mixture. Science 2019, 366, 241. [PubMed: 31601769] (d)Shekhah O; Belmabkhout Y; Chen Z; Guillerm V; Cairns A; Adil K; Eddaoudi M Made-to-order metal-organic frameworks for trace carbon dioxide removal and air capture. Nat. Commun 2014, 5, 4228. [PubMed: 24964404] (e)Cui X; Yang Q; Yang L; Krishna R; Zhang Z; Bao Z; Wu H; Ren Q; Zhou W; Chen B; Xing H Ultrahigh and Selective SO2 Uptake in Inorganic Anion-Pillared Hybrid Porous Materials. Adv. Mater 2017, 29, 1606929.

(14). Elsaidi SK; Mohamed MH; Simon CM; Braun E; Pham T; Forrest KA; Xu W; Banerjee D; Space B; Zaworotko MJ; Thallapally PK Effect of ring rotation upon gas adsorption in SIFSIX-3-M (M = Fe, Ni) pillared square grid networks. Chem. Sci 2017, 8, 2373. [PubMed: 28451342]

(15). O'Nolan D; Kumar A; Zaworotko MJ Water Vapor Sorption in Hybrid Pillared Square Grid Materials. J. Am. Chem. Soc 2017, 139, 8508. [PubMed: 28585820]

(16). Wang X-F; Du C-C; Zhou S-B; Wang D-Z Six complexes based on bis(imidazole/benzimidazole-1-yl)pyridazine ligands: Syntheses, structures and properties. J. Mol. Struct 2017, 1128, 103.

(17). Spek A Structure validation in chemical crystallography. Acta Crystallogr., Sect. D: Biol. Crystallogr 2009, 65, 148. [PubMed: 19171970]

(18). Zhang J-P; Liao P-Q; Zhou H-L; Lin R-B; Chen X-M Single-crystal X-ray diffraction studies on structural transformations of porous coordination polymers. Chem. Soc. Rev 2014, 43, 5789. [PubMed: 24971601]

(19). (a)Deria P; Gómez-Gualdrón DA; Bury W; Schaef HT; Wang TC; Thallapally PK; Sarjeant AA; Snurr RQ; Hupp JT; Farha OK Ultraporous, Water Stable, and Breathing Zirconium-Based Metal–Organic Frameworks with ftw Topology. J. Am. Chem. Soc 2015, 137, 13183. [PubMed: 26387968] (b)Liu D; Liu T-F; Chen Y-P; Zou L; Feng D; Wang K; Zhang Q; Yuan S; Zhong C; Zhou H-C A Reversible Crystallinity-Preserving Phase Transition in Metal–Organic Frameworks: Discovery, Mechanistic Studies, and Potential Applications. J. Am. Chem. Soc 2015, 137, 7740. [PubMed: 26011818]

(20). Groom CR; Bruno IJ; Lightfoot MP; Ward SC The Cambridge Structural Database. Acta Crystallogr., Sect. B: Struct. Sci., Cryst. Eng. Mater 2016, 72, 171.

(21). Gu C; Hosono N; Zheng J-J; Sato Y; Kusaka S; Sakaki S; Kitagawa S Design and control of gas diffusion process in a nanoporous soft crystal. Science 2019, 363, 387. [PubMed: 30679369]

(22). Nugent PS; Rhodus VL; Pham T; Forrest K; Wojtas L; Space B; Zaworotko MJ A Robust Molecular Porous Material with High CO2 Uptake and Selectivity. J. Am. Chem. Soc 2013, 135, 10950. [PubMed: 23859072]

(23). Kondo A; Noguchi H; Ohnishi S; Kajiro H; Tohdoh A; Hattori Y; Xu W-C; Tanaka H; Kanoh H; Kaneko K Novel Expansion/Shrinkage Modulation of 2D Layered MOF Triggered by Clathrate Formation with CO_2 Molecules. Nano Lett 2006, 6, 2581. [PubMed: 17090095]

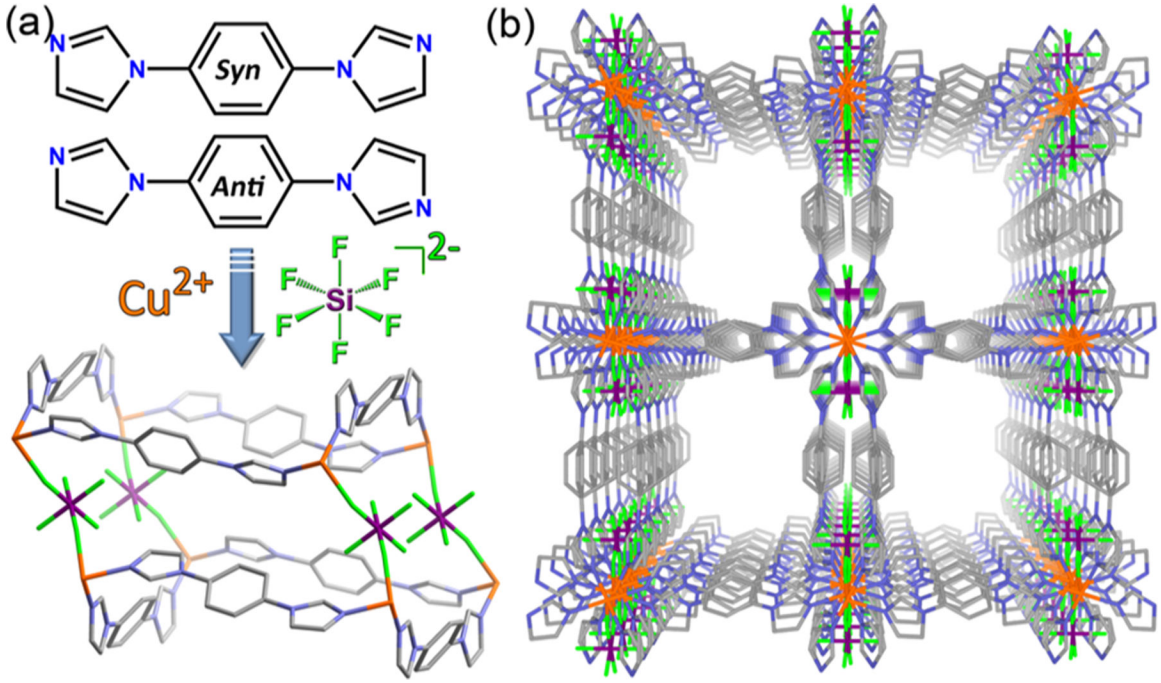

Figure 1.

(**a**) Self-assembly strategy used to design **SIFSIX-23-Cu**. (**b**) 1D channels along the *a*-axis in the as-synthesized form, **SIFSIX-23-Cu-*a***.

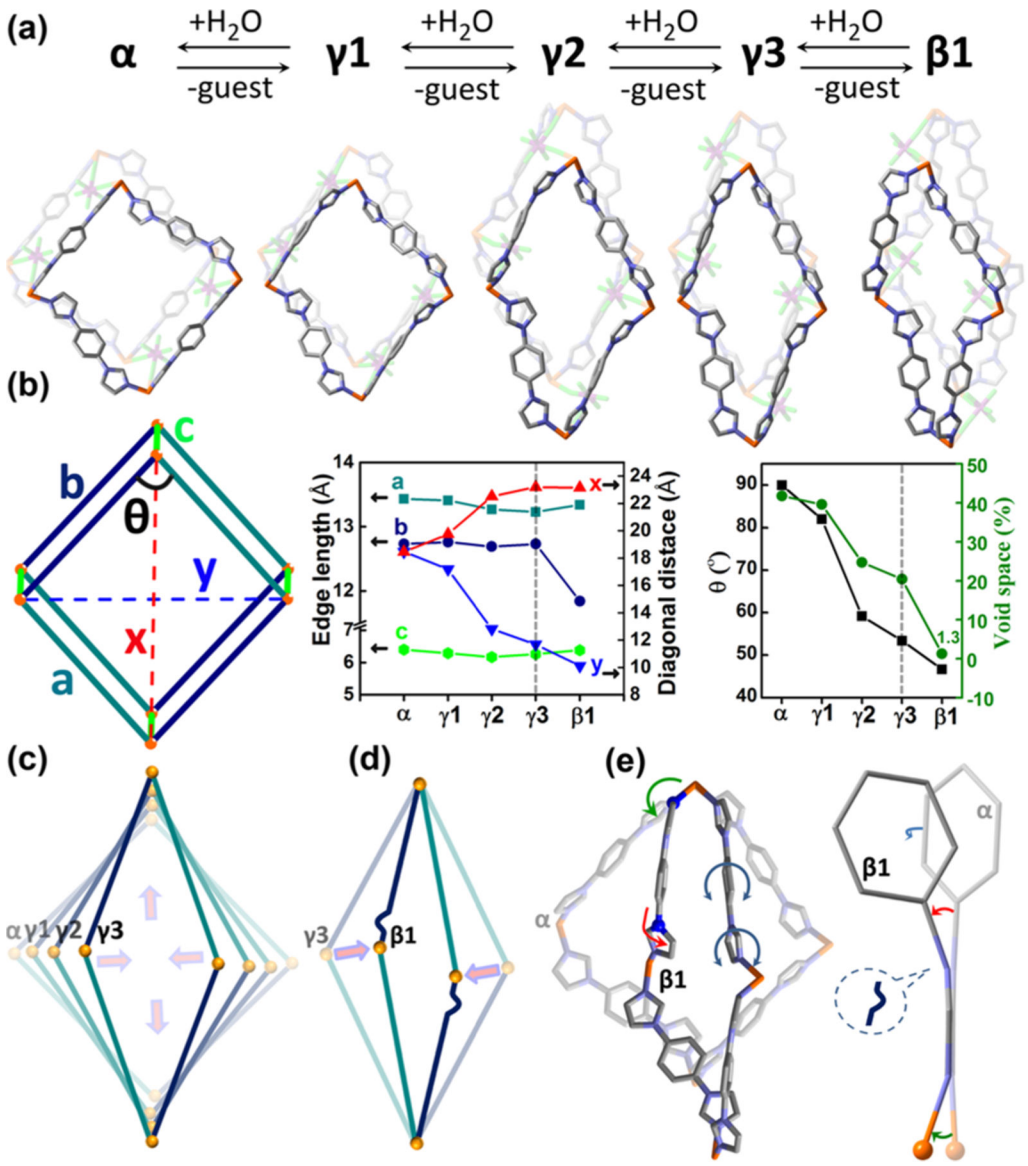

Figure 2.

(a) Guest-induced reversible structural transformations occur between the ***α***, ***γ*1**, ***γ*2**, ***γ*3**, and ***β*1** phases. (b) A parallelogram defines the structural parameters of each phase. Deformation of the parallelogram during the ***α*** to ***γ*3** (c) and the ***γ*3** to ***β*1** (d), transformations. (e) Overlapping parallelograms of the ***α*** and ***β*1** phases highlight structural distortions.

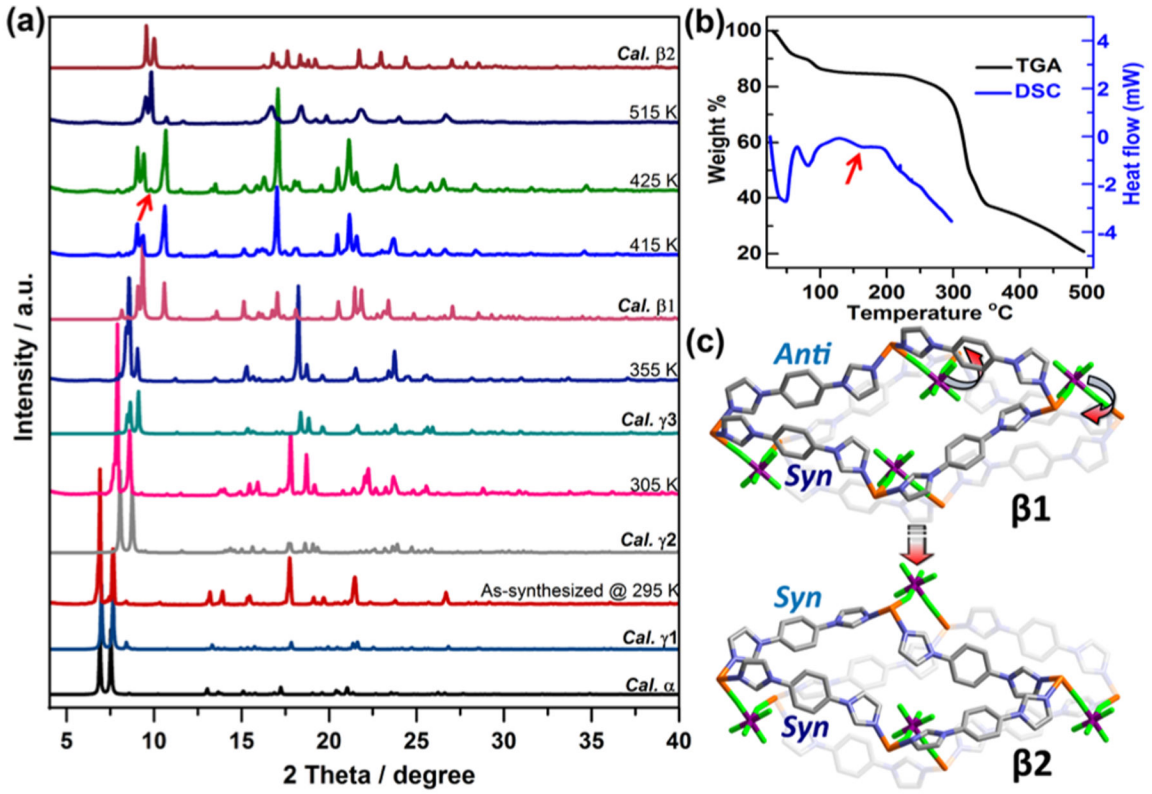

(d)	α	γ1	γ2	γ3	β1	β2
PBE	0.0	14.0	74.5	69.4	107.3	−4.9
PBE−dD sC	0.0	5.6	−2.0	−6.6	−93.3	−221.8

Figure 3.

(a) VT-PXRD of **SIFSIX-23-Cu** from 295 to 515 K. (b) TGA and DSC of **SIFSIX-23-Cu**. (c) Structural changes in the ***β*1** to ***β*2** transformation. (d) Relative energies of the structurally characterized phases (kJ/mol, PBE and PBE-dDsC).

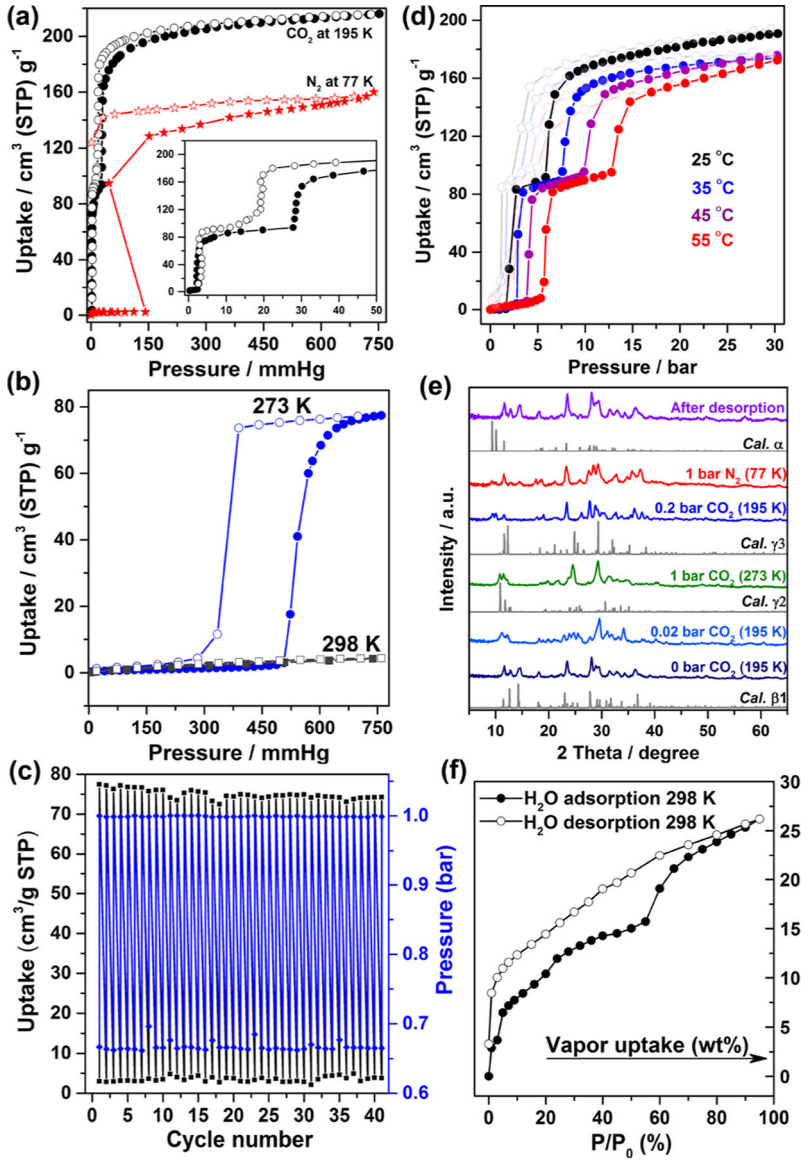

Figure 4.

(a) Gas sorption isotherms of ***β*1** at 195 K (CO_2) and 77 K (N_2). (b) CO_2 sorption isotherms of ***β*1** at 273 and 298 K. (c) Adsorption/desorption cycles of ***β*1** at 273 K. (d) High-pressure CO_2 sorption isotherms at 25 to 55 °C. (e) In situ NPD patterns at various conditions. At 77 K, 1 bar N_2 trace ***β*1** is present because of large sample size (>1 g) and slow kinetics; equilibrium took >24 h. (f) Water sorption isotherm of ***β*1** at 298 K.

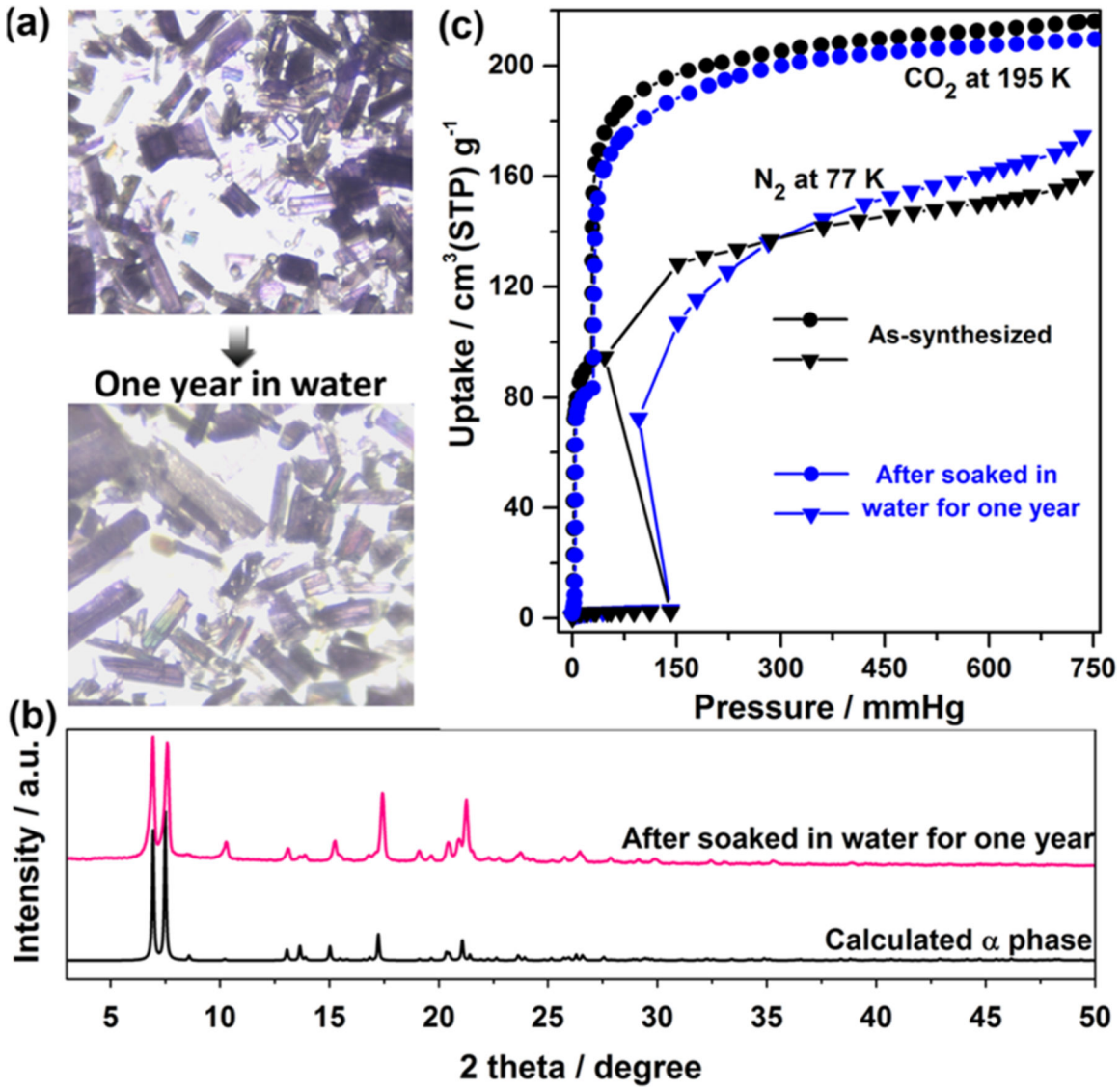

Figure 5.

(a) As-synthesized crystals compared to those soaked in water for one year. (b) PXRD pattern of **SIFSIX-3-Cu** soaked in water for one year compared with that calculated for ***a***. (b) The 195 K CO_2 and 77 K N_2 adsorption isotherms of samples before and after being soaked in water for one year.